

## Intermittency and Structure Functions in Channel Flow Turbulence

F. Toschi,<sup>1,2</sup> G. Amati,<sup>3</sup> S. Succi,<sup>4</sup> R. Benzi,<sup>5</sup> and R. Piva<sup>6</sup>

<sup>1</sup>*Dipartimento di Fisica, Università di Pisa, Piazza Torricelli 2, I-56100, Pisa, Italy*

<sup>2</sup>*INFN, Unità di Tor Vergata, Roma, Italy*

<sup>3</sup>*CASPUR, Università "La Sapienza," Piazzale Aldo Moro 5, I-00185, Roma, Italy*

<sup>4</sup>*Istituto Applicazioni Calcolo "Mauro Picone," Viale Policlinico 137, I-00161, Roma, Italy*

<sup>5</sup>*AIPA, Via Po 14, I-00100, Roma, Italy*

<sup>6</sup>*Dipartimento di Meccanica e Aeronautica, Università "La Sapienza," Via Eudossiana 18, I-00184, Roma, Italy*

(Received 14 July 1998; revised manuscript received 25 February 1999)

We present a study of intermittency in a turbulent channel flow. Scaling exponents of longitudinal streamwise structure functions,  $\zeta_p/\zeta_3$ , are used as quantitative indicators of intermittency. We find that near the center of the channel the values of  $\zeta_p/\zeta_3$  up to  $p = 7$  are consistent with the assumption of homogeneous and isotropic turbulence. Moving towards the boundaries, we observe a growth of intermittency which appears to be related to an intensified presence of ordered vortical structures. We argue that the clear transition in the nature of intermittency appearing in the region close to the wall is related to a new length scale which becomes the relevant one for scaling in high shear flows. [S0031-9007(99)09455-7]

PACS numbers: 47.60.+i, 47.27.Eq, 47.27.Nz, 47.55.-t

Spatiotemporal intermittency is one of the most intriguing properties of fluid dynamics turbulence. Intermittency can be described by means of the scaling behavior of the structure functions  $S_p(r)$  built out of the velocity difference, namely,  $S_p(r) = \langle \delta v(r)^p \rangle$  where  $\delta v(r) = \delta \vec{v}(\vec{r}) \cdot \vec{r}/r$ . In the inertial range,  $S_p(r)$  scale homogeneously with exponents  $\zeta_p$ , i.e.,  $S_p(r) \propto r^{\zeta_p}$ . Intermittency reflects in anomalous values (i.e., different from the Kolmogorov 1941 prediction  $\zeta_p = p/3$ ) of the  $\zeta_p$  (see Frisch [1]). Although many efforts have been devoted to the understanding of intermittency in homogeneous and isotropic turbulence, the case of wall turbulence dominated by very strong shear flow is still under debate. In fact, while the decrease of scaling exponents towards the wall has been recently pointed out by both experimental and numerical investigations [2,3], a physical explanation of this effect is still missing.

The main objective of this paper is to analyze the scaling exponents (if any) and to explore their functional dependence on the nonhomogeneous coordinate. To this purpose, we investigate numerically a channel flow [4,5], possibly the simplest instance of a shear-dominated flow.

The problem of characterizing the complex phenomena arising in the near-wall region, and their relation to the lack of isotropy, has been analyzed in depth by several authors (e.g., see Antonia *et al.* [6] and L'vov and Procaccia [7]). With specific reference to intermittency, Kuznetsov *et al.* [8] presented an experimental investigation of fine-scale structure of turbulence for different shear flows. Even though they recognize that scaling exponents may be different for various flows or various locations of the same flow, they do not seem to address the issue of the spatial dependence of the exponents  $\zeta_p$ . This issue is examined in a recent paper by Camussi *et al.* [9], in which the authors propose a technique to identify co-

herent structures and relate them to the increase of intermittency in (homogeneous and nonhomogeneous) grid turbulence. The present work is fairly distinct in purpose, since we analyze the spatial behavior of the scaling exponents and their link to coarse-grained features of the flow in the near-wall region. Besides the fundamental interest on its own, the existence of such correlation could prove very valuable for the design of more efficient large-eddy-simulation models (see, for instance, Scotti and Meneveau [10]).

We have performed a direct numerical simulation achieving a high statistical accuracy (about  $10^3$  in time units  $U_0/h$ , where  $U_0$  is the centerline velocity and  $h$  is the channel half-width). Numerical simulations have been performed on a massively parallel machine using a LBE (lattice Boltzmann equation) code. The spatial resolution of the simulation was  $256 \times 128 \times 128$  grid points. Periodic boundary conditions were imposed along the streamwise ( $x$ ) and spanwise ( $z$ ) directions, whereas no-slip boundary conditions were applied at the top and the bottom planes (normal to wall direction,  $y$ ). The Reynolds number is  $Re \approx 3000$ . Further details about the numerical scheme can be found in [11] and references therein. In the following we use wall units defined as  $y^+ = y \cdot v^*/\nu$  and  $v^+ = v/v^*$  where  $v^*$  is the friction velocity [12]. In these units, the channel is 640 long, 320 wide, and 320 high.

To study intermittency in the channel, we introduce the following  $y$ -dependent longitudinal streamwise structure functions:

$$S_p(r^+, y^+) = \langle |v_x(x^+ + r^+, y^+, z^+) - v_x(x^+, y^+, z^+)|^p \rangle. \quad (1)$$

The average is taken at a fixed  $y^+$  value (the normal to wall coordinate). The quantities  $S_p(r^+, y^+)$  have been

measured for each value of  $y$ . Our data set allows enough statistical accuracy to estimate  $S_p(r^+, y^+)$  for  $p \leq 7$ . Because of the low Reynolds number, we use extended self-similarity (ESS) [13] in order to extract  $\zeta_p$  values. We remind that ESS consists of measuring structure functions as a function of  $S_3$  rather than in terms of space separation  $r$ . This procedure allows a much better accuracy for the evaluation of the scaling exponents, although it does not provide any estimate of the  $y^+$  dependence of  $\zeta_3$ . In order to compute the scaling exponents  $\zeta_p(y)$  we have analyzed the ESS local slopes  $D_{p,q}(r^+, y^+) = d \log[S_p(r^+, y^+)] / d \log[S_q(r^+, y^+)]$  for each value of the  $y^+$  coordinate. We have found two regions in  $y^+$ , hereafter referred to as region H (“homogeneous”) and region B (“boundary”), respectively, where well defined constant local slopes for the scaling exponents can be detected. Region H is close to the center of the channel ( $y^+ \geq 100$ ) while region B is close to the viscous sublayer ( $20 \leq y^+ \leq 50$ ). In region H, the scaling exponents  $\zeta_p(H)$  are found to be approximately the same as the ones measured in homogeneous and isotropic turbulence. On the other hand, in region B the scaling exponents  $\zeta_p(B)$  have been found to be much smaller than  $\zeta_p(H)$ . Moreover, while in region H the scaling range starts at  $r^+ \geq 25$ , in region B the scaling range starts at  $r^+ \geq 50$ , consistently with previous findings [14]. In the intermediate region between region H and region B, it is difficult to identify a range in  $r$  where a scaling exponent can be defined with enough confidence.

In order to clarify the discussion, we show in Figs. 1 and 2 the local slopes  $D_{6,3}(r^+, y^+)$  and  $D_{4,2}(r^+, y^+)$ , respectively, for  $y^+ = 30, 70, 80, 150$ . In the intermediate region (i.e.,  $y^+ = 70, 80$ ), the analysis in terms of local slope does not provide a well defined scaling exponent since the plateau in  $r^+$  is very short. In Figs. 3 and 4 we show  $\zeta_6/\zeta_3$  and  $\zeta_4/\zeta_2$ , respectively, as a function of  $y^+$  with the associated error bars. The large error bars in the region  $50 \leq y^+ \leq 100$  indicate that scaling exponents defined through  $D_{p,q}(r, y^+)$  are poorly defined and should be considered just as effective exponents obtained by the power law fit of the ESS analysis. The situation described in Figs. 1 and 3 is similar for all the scaling exponents  $\zeta_p$  computed in our analysis. Finally, in Table I, we list the numerical values of the scaling exponents for region B, for region H, and for homogeneous isotropic turbulence [15]. Our results indicate that there is a transition in the nature of intermittency between region H and region B. While in region H intermittency is close to what has been observed in isotropic and homogeneous turbulence, in region B much stronger intermittency is observed, which reflects in lower values of the scaling exponents  $\zeta_p$  for  $p > 3$  and larger ones for  $p < 3$ . Between the two regions, a competition between the two types of intermittency should take place, leading to a poorly defined scaling law.

An important question to be addressed concerns the physical mechanisms which produce much stronger inter-

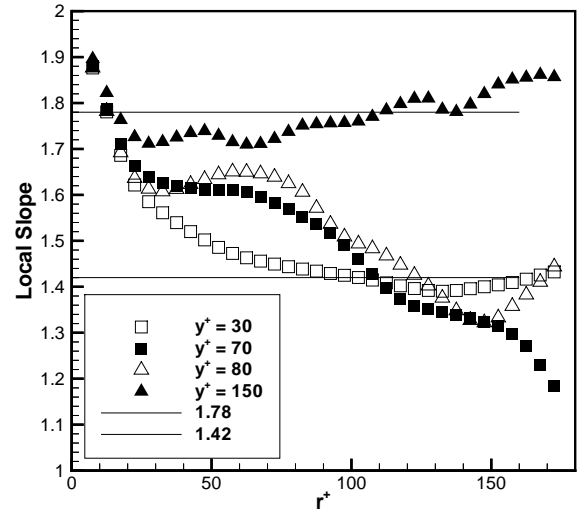


FIG. 1. Local slope  $D_{6,3}$  for four different values of  $y^+$ . The straight lines represent the fit for H and B regions.

mittency in region B with respect to region H. A preliminary answer to this question is given in Fig. 5 where the momentum flux  $\langle v'_x v'_y \rangle$  (a particular component of the Reynolds stress tensor), normalized by its maximum  $\langle v'_x v'_y \rangle_M$ , is shown as a function of  $y^+$ . The momentum flux has a peak within the region B while it goes to zero in region H. This behavior clearly indicates that intermittency grows dramatically in a region characterized by strong mean shear (strong momentum fluxes). The link between momentum flux and the increase of intermittency can be further investigated by looking at the inset of Fig. 5 where we represent  $\zeta_6(y)/\zeta_3(y)$  from Fig. 3 and the rescaled expression

$$\frac{\zeta_6(y^+)}{\zeta_3(y^+)} - \frac{\zeta_6(H)}{\zeta_3(H)} = \left( \frac{\zeta_6(B)}{\zeta_3(B)} - \frac{\zeta_6(H)}{\zeta_3(H)} \right) \frac{\langle v'_x v'_y \rangle}{\langle v'_x v'_y \rangle_M}. \quad (2)$$

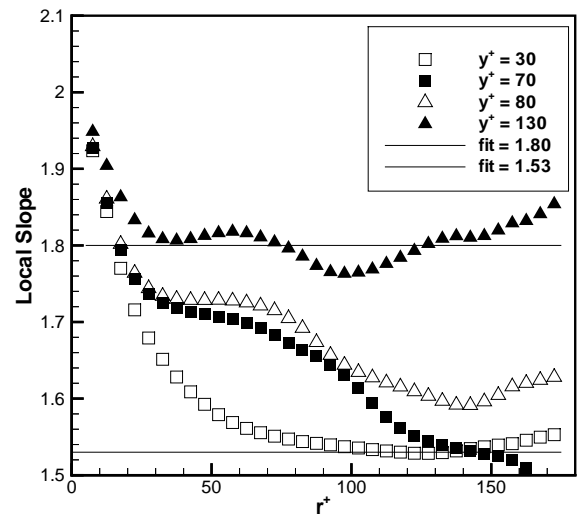


FIG. 2. Local slope  $D_{4,2}$  for four different values of  $y^+$ . The straight lines represent the fit for H and B regions.

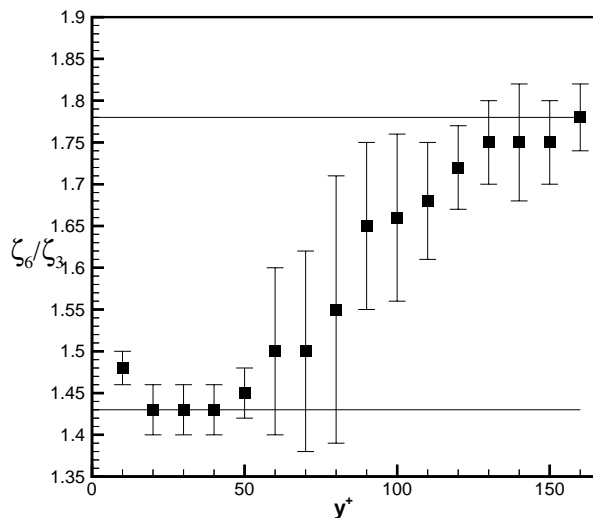


FIG. 3. Scaling exponents  $\zeta_6/\zeta_3$  as a function of  $y^+$ . The straight lines represent the fit for H and B regions.

From Fig. 3, we can argue that the increase of intermittency should be related to the increase of momentum flux and, therefore, to the mean (local) shear.

Moreover, it is well known that turbulent flows near the wall are characterized by well defined coherent structures. In Fig. 5 we show the rms helicity  $h$  ( $h_{\text{rms}} = \langle (\vec{\omega} \cdot \vec{v}) \rangle_{\text{rms}}$ ) as a function of  $y^+$  which is again peaked in region B. Coherent structures carry a significant amount of helicity while dissipation is found to peak in the interstitial region between helicity-carrying structures [16]. Indeed, a clear-cut anticorrelation between helicity fluctuations and dissipation is systematically detected in our numerical simulations. Thus, the alternate presence of regions of high helicity and regions of high dissipation may be responsible for the enhancement of intermittency in region B.

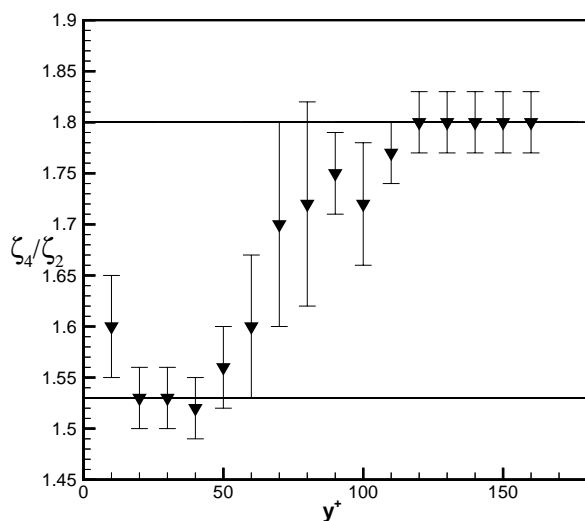


FIG. 4. Scaling exponents  $\zeta_4/\zeta_2$  as a function of  $y^+$ . The straight lines represent the fit for H and B regions.

TABLE I. Normalized scaling exponents in regions H and B for the present simulation, as compared with the values for homogeneous isotropic turbulence  $\zeta_p^{\text{hom}}$  and for a passive scalar  $\zeta_p^{\text{PS}}$ .

$p$	$(\zeta_p/\zeta_3)^{\text{hom}}$	$(\zeta_p/\zeta_3)^{\text{H}}$	$(\zeta_p/\zeta_3)^{\text{B}}$	$\zeta_p^{\text{PS}}$	$\zeta_p^{\text{PS}}/\zeta_3^{\text{PS}}$
1	0.36	0.37	0.44	0.37	0.46
2	0.70	0.70	0.77	0.62	0.77
3	1.00	1.00	1.00	0.80	1.00
4	1.28	1.28	1.17	0.94	1.17
5	1.54	1.54	1.31	1.04	1.30
6	1.78	1.78	1.44	1.12	1.40
7	2.00	2.00	1.55	1.20	1.50

A more quantitative way to investigate the increase of intermittency in region B can be achieved by the following argument. According to the Howarth–Von Karman–Kolmogorov equation for homogeneous shear flows turbulence (see Hinze [17]), one can define a length scale  $L_s(y)$  in terms of the mean energy dissipation  $\epsilon(y)$  and the mean shear  $\Sigma(y)$ , as follows:

$$L_s(y) = \left( \frac{\epsilon(y)}{\Sigma(y)^3} \right)^{1/2}. \quad (3)$$

In the presence of mean shear  $\Sigma$ , for any scale  $r$  we can define two characteristic time scales, namely, the eddy turnover time  $r/\delta v(r)$  and  $1/\Sigma$ . We expect that when the mean shear is large enough, the eddy turnover time is not the relevant time scale for energy transfer from large to small scales. The inequality  $r/\delta v(r) < 1/\Sigma$  gives the range of scales  $r$  where the effect of shear should not be relevant to small scale statistics. By using the

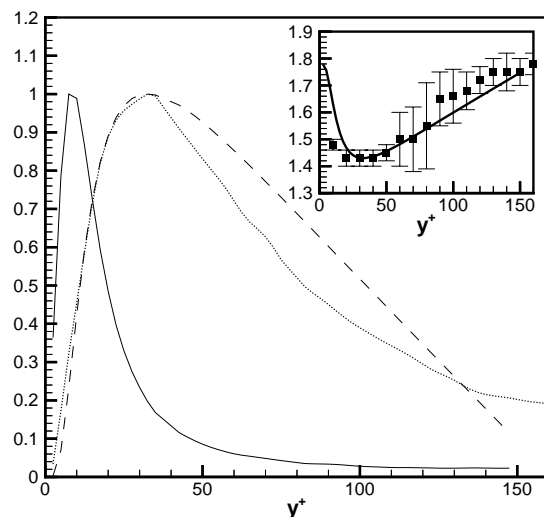


FIG. 5. The momentum flux  $\langle v'_x v'_y \rangle$  (dashed line), normalized by its maximum, is presented together with normalized dissipation (straight line) and rms helicity (dotted line). In the inset the scaling exponent  $\zeta_6/\zeta_3$  is presented together with the rescaled momentum flux as defined by Eq. (2) (continuous line).

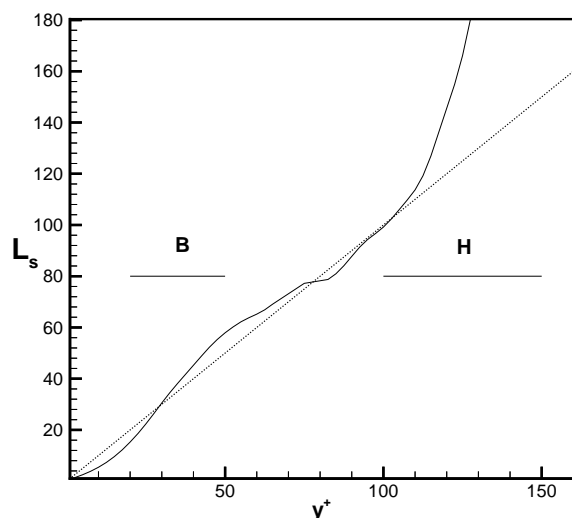


FIG. 6. The characteristic scale  $L_s(y^+)$  is presented as a function of  $y^+$  (continuous line). The dotted line is reported to enlighten the growth of  $L_s$  out of the wall region.

Kolmogorov estimate  $\delta v(r) \sim \epsilon^{1/3} r^{1/3}$ , we find that the above inequality can be written as  $r \leq L_s$ . Thus, for  $r \leq L_s$  one expects that the scaling properties of turbulence are not affected by the mean shear. On the other hand, for  $r \geq L_s$  one expects that the mean shear may significantly change the amount of intermittency. In our numerical simulation  $L_s(y)$  becomes small only in the region B, i.e., where an increase of intermittency is observed (see Fig. 6). This result confirms our finding of a rather clear transition in the physical nature of intermittency, somehow similar to the Bolgiano scaling appearing in the thermal turbulence. Hence, this preliminary analysis seems to indicate that the change of scaling exponents cannot be reduced to a perturbative effect in terms of the mean shear. As a final observation, by inspecting the peak value approached by the  $\zeta_p(y)$  exponents near the wall, we find an interesting similarity with the values,  $\zeta_p^{\text{PS}}$ , pertaining to a passive scalar advected by a turbulent 3D homogeneous and isotropic velocity field [18]. Values of passive scalar  $\zeta_p^{\text{PS}}$  are shown together with our present data in Table I.

Table I suggests that the passive scalar behavior can be traced to these helicity-carrying coherent structures being passively advected by the flow. This observation is in qualitative agreement with the results reported by Pumir and Shraiman [19].

In conclusion, we have rather clear evidence that, in wall bounded turbulence, the increase of intermittency near

the wall is strongly related to the increase of the mean shear. We have introduced a characteristic length scale  $L_s$  induced by the mean shear whose physical meaning is equivalent to the Bolgiano scale for natural convection. Velocity fluctuations at scales  $r \geq L_s$  are observed to be more intermittent than in homogeneous and isotropic turbulence.

The authors thank L. Biferale and C. Casciola for useful hints and suggestions. F. T. acknowledges S. Ciliberto for interesting discussions and for his kind hospitality at ENS-Lyon. This work was partially supported by INFM.

- 
- [1] U. Frisch, *Turbulence* (Cambridge University Press, Cambridge, 1995).
  - [2] G. Amati, F. Toschi, S. Succi, and R. Piva, in *Proceedings of ETC-7*, edited by U. Frish (Kluwer Academic Publishers, Dordrecht, 1998), p. 159.
  - [3] M. Onorato, R. Camussi, and G. Iuso, in *Proceeding of ETC-7* (Ref. [2]), p. 27.
  - [4] J. Kim, P. Moin, and R. Moser, *J. Fluid Mech.* **177**, 133–166 (1987).
  - [5] J. Jimenez and P. Moin, *J. Fluid Mech.* **225**, 213–240 (1991).
  - [6] A. Antonia, J. Kim, and L. B. Browne, *J. Fluid Mech.* **233**, 368–388 (1991).
  - [7] I. Arad, L. Biferale, I. Mazzitelli, and I. Procaccia, *Phys. Rev. Lett.* (to be published).
  - [8] V. R. Kuznetsov, A. A. Praskovsky, and V. A. Sabelnikov, *J. Fluid Mech.* **243**, 595–622 (1992).
  - [9] R. Camussi and G. Guj, *J. Fluid Mech.* **348**, 177–199 (1997).
  - [10] A. Scotti and C. S. Meneveau, *Phys. Rev. Lett.* **78**, 867–870 (1997).
  - [11] G. Amati, S. Succi, and R. Piva, *Int. J. Mod. Phys. C* **8-4**, 869 (1997).
  - [12] L. Landau and E. Lifshitz, *Fluid Mechanics* (Pergamon Press, New York, 1963).
  - [13] R. Benzi, S. Ciliberto, R. Tripiccone, C. Baudet, F. Massaioli, and S. Succi, *Phys. Rev. E* **48**, R29 (1993).
  - [14] G. Amati, S. Succi, and R. Benzi, *Phys. Rev. E* **55**, 1–4 (1997).
  - [15] R. Benzi, L. Biferale, S. Ciliberto, M. V. Struglia, and R. Tripiccone, *Physica (Amsterdam)* **96D**, 162–181 (1996).
  - [16] C. M. Casciola and G. Amati, in *Proceedings of the 8th International Symposium on flow Visualization, Sorrento, 1998* (G.M. Carlomagno, Edinburgh, 1998).
  - [17] O. J. Hinze, *Turbulence* (McGraw-Hill, New York, 1959).
  - [18] Passive scalar values from S. Ciliberto (private communication).
  - [19] A. Pumir and B. I. Shraiman, *Phys. Rev. Lett.* **75**, 3114–3117 (1995).